Acta Biomaterialia 6 (2010) 4229–4237

Contents lists available at ScienceDirect

Acta Biomaterialia

journal homepage: www.elsevier.com/locate/actabiomat

Micropatterning of three-dimensional electrospun polyurethane vascular grafts

Pimpon Uttayarat [a,d], Anat Perets [a,1], Mengyan Li [a,1], Pimchanok Pimton [a], Stanley J. Stachelek [b], Ivan Alferiev [b], Russell J. Composto [c], Robert J. Levy [b], Peter I. Lelkes [a,*]

[a] School of Biomedical Engineering, Science and Health Systems, Drexel University, Philadelphia, PA 19104, USA
[b] Children's Hospital of Philadelphia, University of Pennsylvania, Philadelphia, PA 19104, USA
[c] Department of Materials Science and Engineering, University of Pennsylvania, Philadelphia, PA 19104, USA
[d] Thailand Institute of Nuclear Technology, Bangkok 10900, Thailand

ARTICLE INFO

Article history:
Received 19 December 2009
Received in revised form 4 June 2010
Accepted 8 June 2010
Available online 17 June 2010

Keywords:
Polyurethane graft
Microgrooves
Microfibers
Cell alignment
Human endothelial cells
Electrospinning
Spin casting
Vascular graft

ABSTRACT

The uniform alignment of endothelial cells inside small-diameter synthetic grafts can be directed by surface topographies such as microgrooves and microfibers to recapitulate the flow-induced elongation and alignment of natural endothelium. These surface micropatterns may also promote directional migration and potentially improve anastomotic ingrowth of endothelial cells inside the synthetic grafts. In this paper, we developed electrospinning and spin casting techniques to pattern the luminal surface of small-diameter polyurethane (PU) grafts with microfibers and microgrooves, respectively, and evaluated endothelial cell orientation on these surface micropatterns. Tracks of circumferentially oriented microfibers were generated by electrospinning PU onto a mandrel rotated at high velocity, whereas longitudinal tracks of microgrooves were generated by spin casting PU over a rotating poly(dimethylsiloxane) mold. We found that both PU grafts possessed longitudinal Young's moduli in the range of 0.43 ± 0.04 to 2.00 ± 0.40 MPa, comparable with values obtained from native artery. Endothelial cells seeded onto the grafts formed confluent monolayers with individual cells exhibiting elongated morphology parallel to the micropatterns. The cells were phenotypically similar to natural endothelium as assessed by the expression of the endothelial cell-specific marker, vascular endothelial cell cadherin. In addition, the cells were also responsive to stimulation with the pro-inflammatory cytokine tumor necrosis factor-α as assessed by the inducible expression of intercellular adhesion molecule-1. These results demonstrate that our micropatterned PU grafts possessed longitudinal Young's moduli in the same range as native vascular tissue and were capable of promoting the formation of aligned and cytokine-responsive endothelial monolayers.

1. Introduction

Cardiovascular disease is a major cause of death in the Western society [1,2]. More than one million vascular procedures, including bypass surgery, are performed each year in the USA alone [1]. The procedure typically requires the use of autologous veins (primarily saphenous veins) as bypass conduits to treat occlusion in coronary and peripheral arteries. This bypass surgery often results in secondary morbidity and is not possible in many patients who lack a suitable vein for bypass grafting [2–4]. Due to these limitations in autologous vessels, the use of synthetic vascular grafts has become an attractive "off-the-shelf" alternative as such grafts can be prefabricated to specific dimensions.

Despite clinical success for synthetic grafts with inner diameters larger than 6 mm, small-diameter synthetic grafts (<6 mm) often fail within a short time after bypass surgery due to thrombosis and intimal hyperplasia [2,4–7]. These problems are often caused by the lack of an endothelial coverage on synthetic grafts [8] and the mismatch between the mechanical properties [5,9,10] of synthetic materials and native vascular tissue. In the former case, the absence of endothelial cell ingrowth into the midgraft area can persist even after 10 years post-surgery [8]. Therefore, the development of compliant small-diameter synthetic grafts that promote endothelial cell adhesion is the central focus in most recent studies [4,5,7,11].

Electrospinning is a versatile method to construct three-dimensional (3D) synthetic polymeric grafts [2,4,5,7,12] with mechanical properties comparable to native vascular tissue [5]. In the electrospinning process, fibers with nanometer- to micrometer-scale diameters are generated when a jet of polymeric solution is drawn across an electric field and in the process solidifies on a rotating tubular collector [4,5,11,13]. Depending on the rotational speed of the collector, the electrospun fibers can be organized into a nonwoven mesh [5,7,14] or into oriented patterns [7,11,15]. In addition to the use of elastomeric polymers to match the compliance

* Corresponding author. Tel.: +1 215 762 2071; fax: +1 215 895 4983.
E-mail address: pilelkes@drexel.edu (P.I. Lelkes).
[1] These authors contributed equally to this article.

1742-7061/$ - see front matter © 2010 Acta Materialia Inc. Published by Elsevier Ltd. All rights reserved.
doi:10.1016/j.actbio.2010.06.008

of native vascular tissue, the physical entanglement of polymeric fibers into a 3D matrix has been shown to further increase the grafts' compliance as well as contribute to the healing process [5].

The natural nonthrombogenic property of healthy blood vessels is conferred by endothelial monolayers that line the vessel lumens. Cell-surface interactions play a key role in the formation of endothelial monolayers on synthetic polymer surfaces. Endothelial cells have been shown to recognize and respond to the presence of micropatterns on their underlying substrata. Previous studies on synthetic surfaces have shown that surface topographies such as pores [1,16–18] and meshes [7,14] effectively stimulate spreading, adhesion and proliferation of endothelial cells, whereas oriented fibers [7] and grooves [6,19] induced a uniform cell alignment on the surface. In our previous work [20] we found that the grooved patterns induced the uniform alignment of bovine aortic endothelial cells as well as directional cell migration even in the presence of physiological shear stress. Thus, well-defined tracks such as microgrooves on the synthetic grafts' lumen can potentially improve the anastomotic ingrowth of endothelial cells and subsequent formation of an endothelial monolayer.

In this paper, we used electrospinning and spin casting to pattern the luminal lining of small-diameter polyurethane (PU) grafts with microfibers and microgrooves, respectively, and compared their ability to promote endothelial cell alignment as well as their contribution to the graft's compliance. The alignment of individual cells parallel to tracks of microfibers and microgrooves persisted at confluence on both micropatterned surfaces. In addition, PU grafts fabricated by either technique exhibited Young's moduli in the longitudinal direction similar to the values obtained from native aorta and could withstand a uniaxial strain of up to 300%. Lastly, the cells maintained their response to stimulation by tumor necrosis factor-α (TNF-α) as shown in the increase of intercellular adhesion molecule-1 (ICAM-1), a key indicator of inherent endothelial physiology. Collectively, the micropatterns investigated in our study can be applied to the fabrication of novel small-diameter synthetic grafts that are capable of guiding cellular alignment while maintaining quasi-endogenous responsiveness of the endothelial monolayer.

2. Materials and methods

2.1. Electrospinning of polyurethane

Tecothane, an aromatic polyether polyurethane, was obtained from Thermedics Inc. (Woburn, MA), purified and characterized as previously reported [21]. Solutions of 5% (w/v) PU were made for electrospinning by dissolving lyophilized PU in 1,1,1,3,3,3-hexafluoro-2-propanol (Sigma), with stirring for 2 h at 40 °C and then overnight at room temperature. This PU concentration was established in preliminary studies in our laboratory to generate continuous bead-free microfibers.

A horizontal electrospinning apparatus was setup inside a chemical hood as shown in Fig. 1. The power supply (ES30-0.1P, Gamma High Voltage Research) was set to 12 kV and the distance between the reservoir of the PU solution and the target that collected the electrospun fibers was kept constant at 12 cm. The PU solution inside a syringe was fed at 0.8 ml h^{-1} by an infusion pump (KD Scientific Infusion Pump, Fisher) through a blunt 18 gauge stainless steel needle towards the target. To investigate the optimal PU concentration that yielded continuous microfibers, glass coverslips were placed on the flat copper target to collect electrospun fibers.

To fabricate PU grafts with circumferentially aligned microfibers by electrospinning (electrospun grafts), the copper plate was replaced with a high-speed rotating drill (Dremel). An aluminum (Al) mandrel was machined to 4 mm in diameter and 5 cm in length by the Drexel University Instrumentation Shop. During electrospinning, the Al mandrel was set to rotate at 35,000 rpm while collecting electrospun fibers. About 2 ml of 5% PU solution was used to fabricate one graft. After drying inside a hood overnight, PU grafts were released from the mandrel. The fiber dimension as well as graft thickness were examined and measured by scanning electron microscopy (SEM).

For the fabrication of PU grafts with luminal lining of microgrooves, a mold consisting of microgrooves (3.6 μm channel × 3.3 μm ridge × 1 μm depth) was first fabricated on a silicon wafer and then transferred to poly(dimethylsiloxane) (PDMS; Robert McKeown, Inc., Branchburg, NJ), as previously described [6]. This micropatterned PDMS sheet (2.5 × 2.5 cm^2 and 200 μm thick) was wrapped around a mandrel with the microgrooves aligned parallel to the mandrel length and secured with nail polish to create a 3D mold with a grooved surface exposed to air. Approximately 1 ml of 3% PU solution was spun cast on the slowly rotating mandrel (50 rpm) under a high-intensity halogen lamp (300 W) for 10 min to transfer the microgroove patterns from PDMS to PU. Immediately following the spin casting process, the 1 ml of 5% PU solution was electrospun onto the mandrel while rotating at 50 rpm. The resulting grafts were referred to as hybrid grafts. Both luminal and outer surfaces were then examined by SEM.

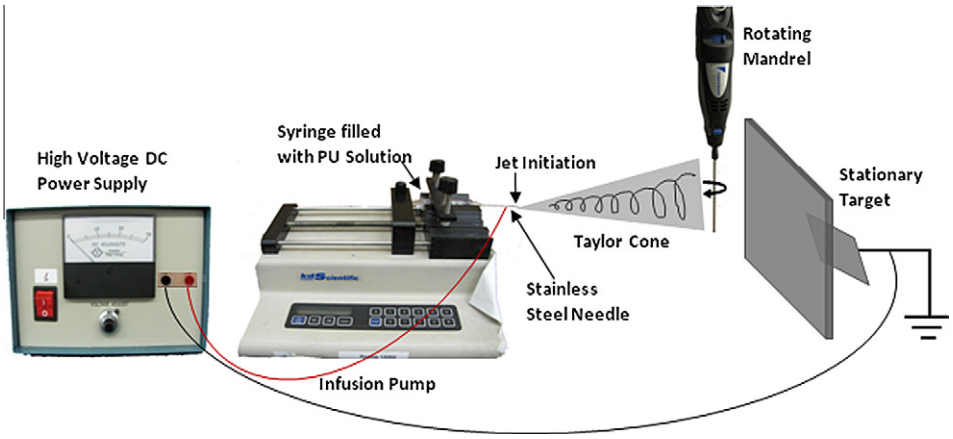

Fig. 1. Schematic of electrospinning setup. The electrospinning apparatus consists of (1) a high voltage DC power supply, (2) an infusion pump, (3) a syringe filled with PU solution that is attached to (4) a stainless steel needle, (5) a rotating mandrel and (6) a stationary target connected to the ground. The power supply generates an electric field between the needle and mandrel. The infusion pump drives a constant flow of PU solution, which forms a Taylor cone at the needle tip under the electric field, to solidify on the mandrel. For electrospun grafts, the mandrel is rotated at 35,000 rpm to generate circumferentially oriented microfibers along the mandrel. For hybrid grafts, a PDMS mold embedded with microgrooves is wrapped around the mandrel to replicate a microgroove pattern parallel to the mandrel's long axis onto the graft lumen.

2.2. Uniaxial tensile test

The elastic moduli of PU grafts were determined by a uniaxial stretching test (Instron model 5564 with the Merlin version 9.0 software, Department of Materials Science and Engineering, University of Pennsylvania). For electrospun grafts, each graft was cut circumferentially (parallel to the fiber direction) and longitudinally (orthogonal to the fiber direction) with respect to the graft length into rectangular specimens (0.6 cm width × 1.2 cm length for the first case and 1.2 cm width × 2.5 cm length for the latter). The graft thickness was determined by SEM. Native aortas were harvested from healthy adult rabbits in accordance with a Drexel University IACUC-approved protocol, stored in normal saline and tested under uniaxial stretching within 2 h of harvest. The crosshead speed was set at 5 mm min^{-1} on the 0.1 N load transducer. Each specimen was strained to 50% from its original length for 10 cycles and then to 300% to test whether it could withstand the tensile force or not. Data were recorded as load and displacement.

2.3. Cell culture

Bovine aortic endothelial cells (BAECs) were isolated and cultured in gelatin-coated T75 flasks using Dulbecco's modified Eagle's medium (DMEM; Mediatech) supplemented with 10% fetal bovine serum (FBS; Hyclone), 1 mg ml^{-1} glucose, 0.3 mg ml^{-1} L-glutamine, 10 μg ml^{-1} streptomycin, 10 U ml^{-1} penicillin and 25 ng ml^{-1} amphotericin (complete DMEM). Cells were sub-cultured every 2 days and used at passages 8–12. Human umbilical vein-derived EA.hy926 endothelial cells were kindly provided by Professor Cora-Jean Edgell at the University of North Carolina, Chapel Hill. Cells were kept in culture in gelatin-coated T75 flasks using DMEM supplemented with 10% FBS, 4.5 mg ml^{-1} glucose, 100 μg ml^{-1} streptomycin and 100 U ml^{-1} penicillin. Cells were sub-cultured every 2 days and cell passages 30–42 were used in all experiments. The endothelial phenotype (as inferred from, e.g., morphology, rate of proliferation, cytokine responsiveness, uptake of acetylated LDL and vascular endothelial cell cadherin (VE-cadherin) expression) of BAECs (at passages <15) and of EA.hy926 cells (at passages <50) has been established previously in our laboratory. For extended culture periods of up to 7 days, the cells were maintained at 37 °C and 95% relative humidity in a 5% CO_2 incubator with fresh medium being added to the culture every day.

2.4. Endothelialization of PU grafts

Before cell seeding, PU grafts were sterilized by immersion in a solution containing streptomycin, penicillin and amphotericin (Mediatech). To promote initial endothelial cell attachment on PU grafts, all graft samples were incubated in 10 μg ml^{-1} fibronectin (Fn; Sigma) solution overnight and non-specific adhesion was blocked in 1% bovine serum albumin (BSA; Sigma) solution as previously described [6].

PU grafts were placed inside bioreactors adapted from 3 ml syringes that were capped with lure locks and plungers. BAECs and EA.hy926 endothelial cells were harvested at 90% confluence and resuspended in DMEM supplemented with 25 mM HEPES (Mediatech). One million cells in 2 ml of culture medium were added to each syringe. All syringes were rotated on an orbital shaker at 37 °C for 2 h with manual rotation about the long axis every 5 min. Following this initial cell seeding step, each graft was then transferred to a T25 flask filled with complete DMEM or fixed in 4% formaldehyde (Fisher) and labeled with TRITC-conjugated phalloidin using a method described in the following section to visualize cell distribution.

2.5. Fluorescence imaging of endothelial monolayer

To visualize the formation of confluent monolayers on the lumen of PU grafts, BAECs and EA.hy926 endothelial cells were immunostained for the endothelial cell-specific marker VE-cadherin or fluorescently labeled with TRITC-conjugated phalloidin for actin filaments [22]. For the immunostaining with VE-cadherin, the cells were fixed in cold (−20 °C) methanol for 5 min, rinsed with PBS and stained with a VE-cadherin-specific antibody (1:40 dilution in PBS, Santa Cruz Biotechnology, Inc., Santa Cruz, CA) for 1 h at room temperature. Excess antibody was removed by three washes in PBS, and specific binding was visualized using A488 chicken anti-goat IgG secondary antibody (1:1000 dilution in PBS, Molecular Probes, Eugene, OR). To visualize actin filaments, the cells were first fixed in 4% formaldehyde at room temperature for 15 min. The cells were then washed, permeabilized with 0.1% Triton and fluorescently labeled with TRITC-conjugated phalloidin (1:200 dilution, Sigma–Aldrich). Vectashield with DAPI (Vector Lab, Burlingame, CA) was then added to each sample before it was mounted on glass slide and enclosed with a coverslip. Fluorescence images were then taken by a conventional upright fluorescence microscope (Leica DMRX).

2.6. Imaging of micropatterns and endothelial monolayer by scanning electron microscopy

The topography of microgrooves and microfibers on the lumen of PU grafts and the presence of an endothelial monolayer were visualized by SEM (FEI XL30, Drexel University). The cross-section (orthogonal to the graft length) and the luminal surface of the graft was mounted on aluminum stubs before being sputter-coated with platinum. For grafts seeded with endothelial cells, the samples were fixed after 5 days in culture with 2% gluteraldehyde at 4 °C for 45 min, rinsed once with sodium cacodylate buffer and then rinsed again with tissue culture-grade water. The cells were then dehydrated sequentially in water–ethanol solutions containing 5%, 30%, 50%, 75% and 90% ethanol and twice in 100% ethanol. The samples were then critical point dried by CPD 7501 (SPI Supplies, Westchester, PA) and visualized by SEM at the acceleration voltage of 10 keV (5 keV in some cases) and working distance of 15 mm.

2.7. ICAM-1 expression

When activated by inflammatory reagents, endothelial cells upregulate leukocyte-endothelial cell adhesion molecules such as ICAM-1 to initiate the inflammatory process [23–25]. In this study, we used ICAM-1 as a marker to assess the response of endothelial cells grown on our polyurethane. To this end, we introduced the pro-inflammatory cytokine TNF-α (Sigma) into EA.hy926 cultures, which has been shown to induce the upregulation of ICAM-1 [24,26].

EA.hy926 endothelial cells were cultured on cast PU films without Fn coating in 24-well tissue culture plates. At 1 day post-confluence, the cells were incubated for 16 h with TNF-α at concentrations of 0 (control) and 10 ng ml^{-1}. This latter concentration of TNF-α has shown to be effective in inducing the expression of ICAM-1 in our preliminary experiments (data not shown). Approximately 5×10^5 cells from each treatment were harvested in 0.005% Trypsin–EDTA solution (Sigma) and resuspended twice in cold PBS with 20 mM EDTA and 1% BSA (blocking buffer) at 4 °C for 5 min (Labofuge 400, Thermo Scientific). The cells were then incubated in phycoerythrin anti-human CD54 or with an isotype control antibody (1:5 dilution, eBioscience) for 30 min on ice, followed by three resuspensions in blocking buffer. For all experiments, 50,000 events per sample were collected for analysis on a

BD FACSCanto flow cytometer (San Jose, CA) using FACSDiva software. To quantify the response of endothelial cells to TNF-α, ICAM-1 expression was analyzed by FlowJo software (Treestar, Ashland, OR, USA) from three independent experiments.

2.8. Data analysis

For electrospun and hybrid grafts, the dimensions of microfibers, ridges, channels, channel depths and graft thicknesses were determined from 5 to 8 SEM images for each sample. To determine the Young's moduli of the fabricated PU grafts, 3–5 specimens for each of the electrospun and hybrid grafts were tested via Instron under tensile mode. In order to assess the alignment of cell shape on microfibers or microgrooves, we defined the cells as being aligned with the micropatterns if their major axes were within ±20° of the microfibers and microgrooves [6]. To determine cell density, cells were counted from images of fluorescently labeled cell nuclei taken from three or four different fields for each sample at indicated time points. Data are expressed as mean ± standard error of mean unless stated otherwise. Statistical analysis was performed by one-way analysis of variance, followed by a post hoc Tukey's *t*-test, with $p \leqslant 0.05$ being statistically significant.

3. Results

3.1. Morphology of micropatterned small-diameter PU grafts

Electrospinning and spin casting techniques were used in our fabrication procedure to produce small-diameter PU grafts with

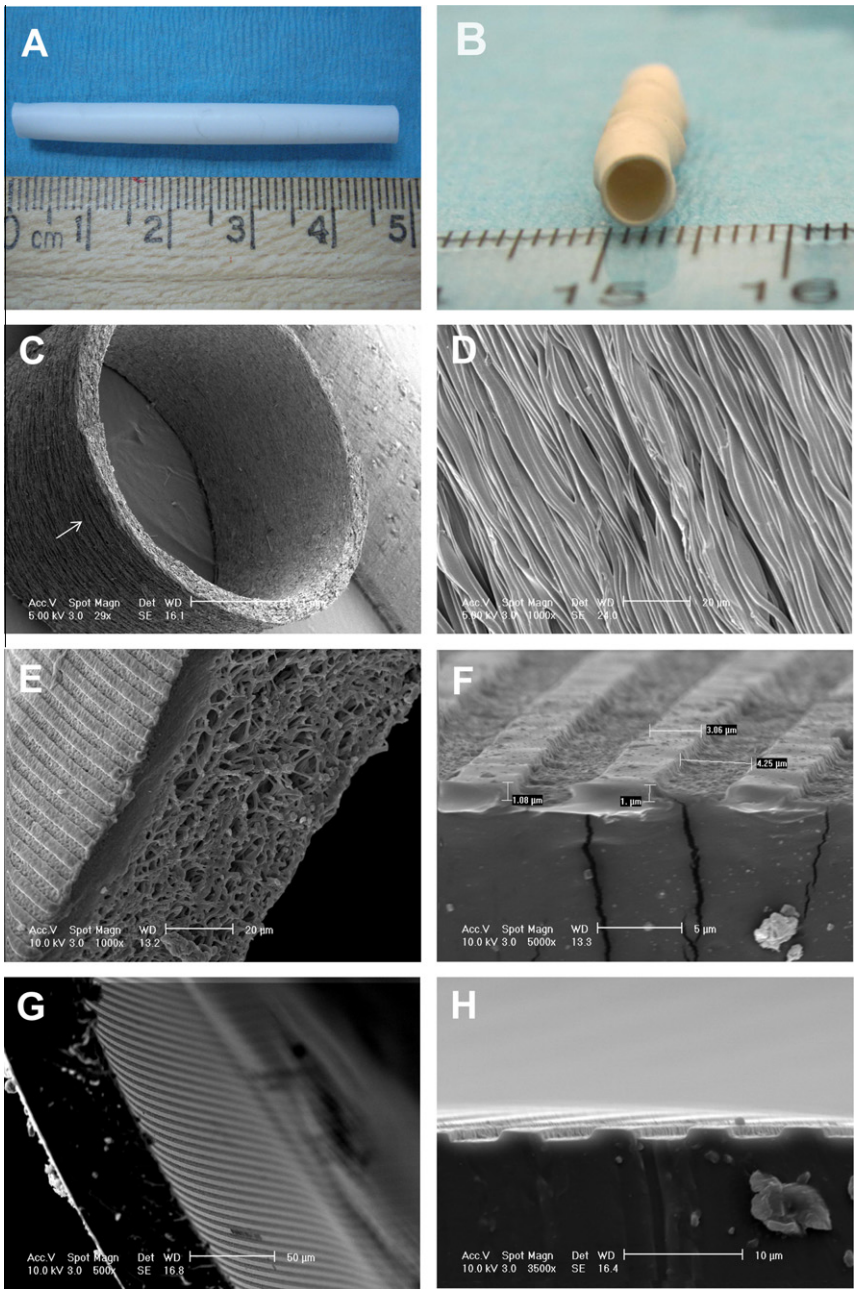

Fig. 2. Small diameter PU grafts fabricated by electrospinning resulting in (A) a graft length of 48 mm and (B) a graft diameter of 4 mm. (C, D) SEM images of electrospun graft showing the arrangement of microfibers that wind circumferentially (arrow) around the graft. (D) Individual microfibers taken from the graft exterior in (C) are shown to be tightly packed and aligned. (E, F) SEM images of hybrid graft consisting of microgrooves on the lumen and mesh of microfibers on the exterior. (G, H) SEM images show a PU graft generated by spin casting alone. The ridge width, channel width and channel depth were 3.6 ± 0.2, 3.9 ± 0.1 and 0.9 ± 0.03 µm, respectively, in (F) and (H).

two distinct micropatterns on their luminal surfaces as shown by SEM (Fig. 2A and B; 48 mm length, ~4 mm inner diameter). Electrospinning of PU solutions onto the fast rotating mandrel (35,000 rpm) resulted in a formation of electrospun grafts that were entirely composed of circumferentially aligned microfibers (Fig. 2C and D) with a mean fiber diameter of 1.20 ± 0.31 μm. The wall thickness of electrospun grafts was 193.3 ± 12.3 μm. By contrast, a combination of spin casting and electrospinning methods resulted in the formation of hybrid grafts composed of different micropatterns on the lumen and on the exterior. Longitudinally oriented microgrooves were generated on the luminal surface by the spin-casting process, whereas the exterior was covered with a mesh of nonwoven fibers generated by electrospinning (Fig. 2E and F). The generation of a nonwoven mesh as opposed to aligned fibers when electrospinning the hybrid graft was due to the much slower speed of the rotating mandrel (50 rpm) required to prevent the PDMS mold from unwinding from the mandrel. The total wall thickness of hybrid grafts was 59.4 ± 1.3 μm where the mesh of microfibers on the exterior accounted for the majority of the graft thickness.

By spin casting PU solution on the rotating mold, the groove dimensions of the original PDMS mold (3.6 μm channel × 3.3 μm ridge × 1 μm depth) were successfully replicated on the luminal surface of hybrid grafts. These microgrooves on the lumen were continuous with the nonwoven mesh of microfibers on the exterior, thus two distinct micropatterns were completely merged together during the fabrication process. The rough appearance of the surface of these microgrooves (Fig. 2F) compared to those of grafts produced by spin casting alone (Fig. 2G and H) is likely due to the shortened solvent evaporation time between spin casting and electrospinning steps. Based on these results, we conclude that microfibers and microgrooves can be patterned on the luminal surface of small-diameter grafts by electrospinning and spin casting techniques, respectively.

3.2. Mechanical properties of PU grafts

The mechanical properties of electrospun and hybrid PU grafts were determined by a uniaxial tensile test. The Young's modulus was determined from the slope of the linear portion of the stress–strain plot for each sample and is tabulated in Table 1. For hybrid grafts, the Young's modulus measured in the longitudinal direction (parallel to the graft length) was 2.0 ± 0.4 MPa. This value was in the range with the Young's modulus of a 2D electrospun PU sheet consisting of an isotropic, nonwoven mesh of microfibers (Table 1). For PU grafts generated by eletrospinning, the grafts exhibited anisotropic moduli due to the circumferential orientation of microfibers. Longitudinally, the Young's modulus was 0.43 ± 0.04 MPa, whereas it increased eightfold to 3.43 ± 0.98 MPa when measured in the circumferential direction parallel to the microfibers. For comparison, the Young's modulus of rabbit aorta measured in the longitudinal direction was 0.50 ± 0.05 MPa. Thus, despite the anisotropy in the electrospun graft's compliance, the Young's modulus measured in the longitudinal direction remains very close to that of native vascular tissue. Based on our fabrication methods, both electrospun and hybrid PU grafts possess the longitudinal Young's moduli that lie within the same range as the native aorta.

The stress–strain plot (Fig. 3) showed that electrospun grafts could withstand tensile loading (solid line) applied parallel to the graft's longitudinal axis (perpendicular to aligned microfibers) up to 300% strain without failure. An inflection was observed in the slope of the stress–strain curve of the electrospun grafts at about 150% strain. The ability of electrospun grafts to sustain large strain deformation is similar to what was observed for the 2D nonwoven PU mesh (dashed line) despite the orientation of microfibers that align perpendicular to tensile load.

Table 1
Young's moduli of polyurethane sheet and grafts characterized by uniaxial tensile test.

	Elastic modulus (MPa)
Nonwoven sheet	1.25 ± 0.28
Electrospun graft	
Longitudinal	0.43 ± 0.04
Circumferential	3.43 ± 0.98
Hybrid graft	2.00 ± 0.40
Rabbit aorta	0.50 ± 0.05

Values are means ± standard error of the mean. For electrospun grafts with unidirectionally orientated microfibers, Young's moduli were determined in both the longitudinal (orthogonal to aligned microfibers) as well as the circumferential (parallel to aligned microfibers). For hybrid grafts and rabbit aortas, the Young's moduli were measured in the longitudinal direction.

In one set of experiments in which electrospun grafts were sutured to rabbit aortae we found that the aortae did indeed break at such high strain (data not shown). Because the electrospun grafts did not break during the tensile test in this study, we only report the elastic moduli of the grafts and not the elongation at break nor the ultimate tensile stress.

After tensile testing, the SEM image showed that the majority of microfibers lost their circumferential alignment (Fig. 3A) and became randomly oriented. Although most electrospun microfibers lost their initial orientation, a few microfibers maintained their circumferential alignment perpendicular to the tensile load (Fig. 3B, arrows). By contrast, all microfibers maintained their circumferential alignment and a few formed bundles when the load was applied parallel to the microfibers' orientation in the circumferential direction (data not shown). Despite the change in the fiber orientation, the grafts could still withstand tensile load up to 300% strain, which is far beyond the physiological strain [27,28], while maintaining their structural integrity. In addition, the grafts also sustained a repetitive tensile test up to 50% strain for 10 cycles. Our results demonstrate that the reorganization of microfibers is able to support the graft's deformation without failure.

3.3. Formation of endothelial monolayers and cellular alignment on PU graft

The biocompatibility of synthetic PU grafts was assessed by the ability of endothelial cells to form a monolayer on the luminal lining. Using a cell seeding system composed of a syringe-based bioreactor and an orbital shaker, we obtained a uniform cell density for both BAECs and EA.hy926 endothelial cells inside electrospun and hybrid grafts. Fig. 4 shows representative images of BAECs grown on the lumens of both grafts. The uniform distribution and alignment of BAECs was observed within 2 h post-seeding (Fig. 4A), on day 3 (Fig. 4B) and when the cells reached confluence on day 5 (Fig. 4C) inside electrospun grafts patterned with microfibers. Similar results were observed in BAECs cultured on hybrid grafts patterned with microgrooves (Fig. 4D, day 3, and Fig. 4E, confluence; see also Ref. [6]). The uniform distribution and alignment of EA.hy926 endothelial cells are also shown in the insets (Fig. 4A, D and E).

The presence of unidirectional surface topography on the lumens of PU grafts can provide contact guidance [6,29,30] to direct the alignment of endothelial cells. We found that most cells (>90%) elongated their cell shape and aligned within 20° parallel to the microfibers and microgrooves (double-headed arrow). At confluence, individual BAECs (Fig. 4C) and EA.hy926 endothelial cells (Fig. 4E, inset) in the monolayer maintained their alignment with the oriented microfibers and microgrooves, respectively, as shown

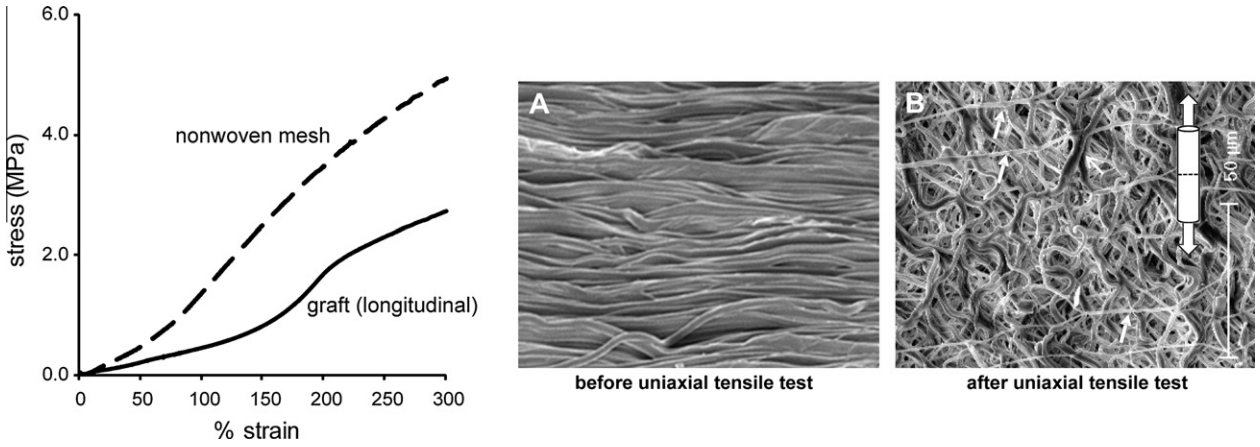

Fig. 3. Stress–strain plot and morphology of electrospun PU grafts. The stress–strain plot is representative of an electrospun graft subjected to a uniaxial tensile test in the longitudinal direction (orthogonal to circumferentially aligned microfibers). SEM images show the organization of microfibers (A) before and (B) after the uniaxial tensile test. The schematic in (B) represents the direction of tensile load acting on the electrospun graft. Arrows in (B) indicate microfibers that maintained their circumferential alignment perpendicular to the tensile load. The scale bar of 50 µm applies to the SEM images in both (A) and (B).

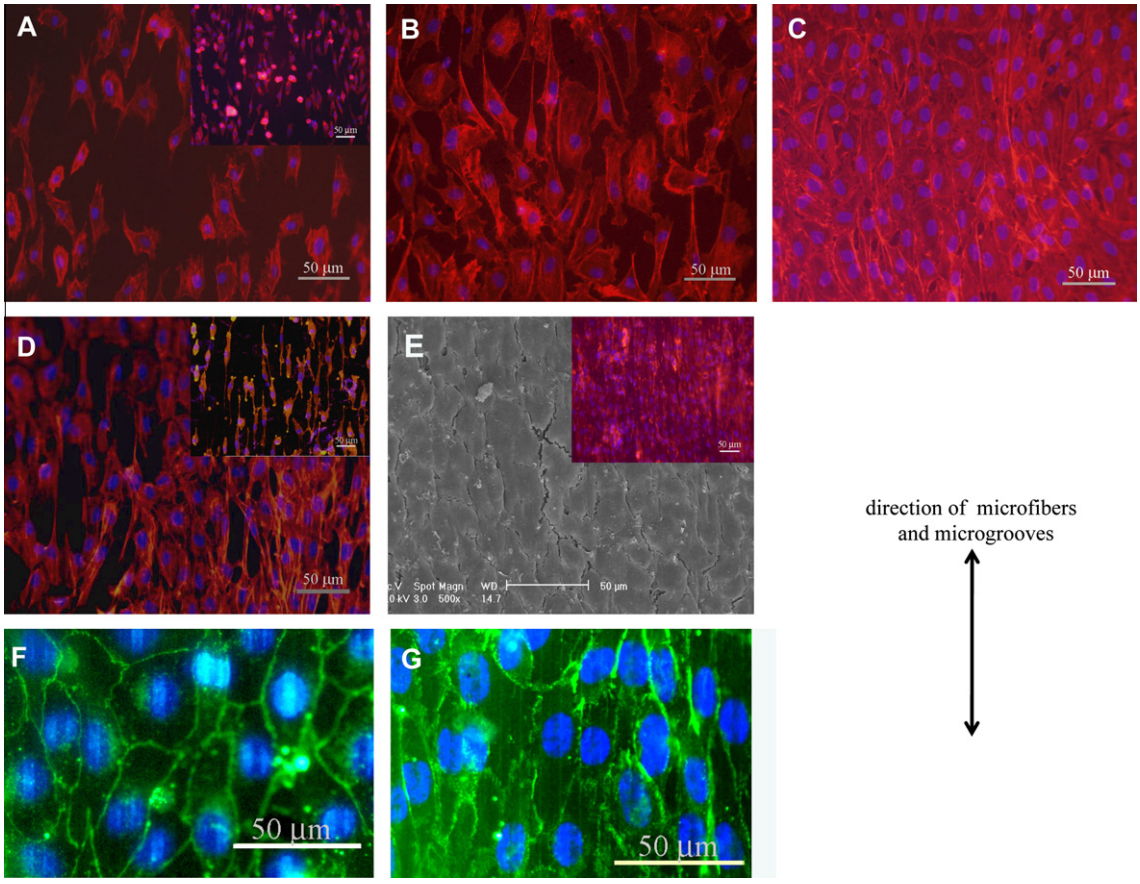

Fig. 4. Morphology of endothelial cells lining micropatterned grafts. (A–C) Cells cultured inside electrospun grafts patterned with microfibers. Overlays of fluorescently stained actin filaments (red) and cell nuclei (blue) of BAECs or EA.hy926 endothelial cells (inset) at (A) 2 h, (B) day 3 and (C) day 5 post-seeding. (D, E) Cells cultured inside hybrid grafts patterned with microgrooves. (D) Overlaid fluorescence image of BAECs or EA.hy926 endothelial cells (inset) at day 3 post-seeding. (E) SEM image of a BAEC monolayer at confluence and overlaid fluorescence image of a EA.hy926 endothelial cell monolayer (inset). (F, G) VE-cadherin staining (green) of (F) BAEC and (G) EA.hy926 monolayers on microgrooves at day 7 post-seeding. Double-headed arrows indicate the direction of microfibers and microgrooves. (For interpretation of the references to colour in this figure legend, the reader is referred to the web version of this article.)

by fluorescence microscopy and SEM microscopy (Fig. 4E, BAECs). The phenotype of endothelial cells grown on hybrid grafts was confirmed by VE-cadherin staining for both BAECs (Fig. 4F) and EA.hy926 endothelial cells (Fig. 4G) at day 7 post-seeding. Similar results were also obtained for electrospun grafts (data not shown).

The proliferation of both BAECs and EA.hy926 endothelial cells cultured on electrospun PU grafts was confirmed by an increase in cell density until the cells reached confluence at day 5 (Fig. 5). Similar results were observed for the cells cultured on hybrid grafts (data not shown). Therefore, endothelial cells can proliferate on syn-

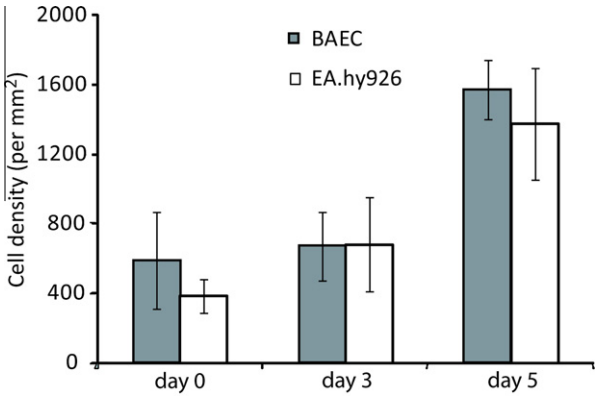

Fig. 5. Endothelial cell growth on electrospun PU grafts. The cell density at different culture times is given as the number of cells per 1 mm^2 area. BAECs (filled bars) and EA.Hy926 (open bars) were counted at the indicated time-points from fluorescently labeled cell nuclei as explained in Section 2. Data are the mean value of counts ± standard deviation.

thetic PU grafts patterned with microfibers and microgrooves and maintain their cellular alignment at confluence.

3.4. ICAM-1 expression by TNF-α treated endothelial cells cultured on tecothane-derived PU

Natural endothelium can be activated by pro-inflammatory cytokines to express the cell surface marker ICAM-1 [24]. To test whether endothelial cell monolayers grown on our tecothane-derived PU could respond in a similar manner, EA.hy926 endothelial cells were cultured on PU in the presence of TNF-α, and ICAM-1 expression was subsequently evaluated by flow cytometry. After incubation with 10 ng ml^{-1} TNF-α for 16 h, EA.hy926 exhibited a 44-fold increase ($p < 0.05$) in ICAM-1 expression compared to the non-treated cells (Fig. 6). Our results indicate that the endothelial cells cultured on tecothane-derived PU are responsive to pro-inflammatory cytokines such as TNF-α, similar to cytokine challenged endogenous endothelia.

4. Discussion

Endothelialization of synthetic vascular grafts remains a central approach in the development of nonthrombogenic, polymer-based blood conduits. Despite the successful attachment of endothelial cells to various chemically modified synthetic grafts in vitro, anastomotic endothelial ingrowth into the midgraft area has not been achieved in clinical trials and animal models [8]. This denuded portion of the graft can result in thrombosis post-bypass surgery. Furthermore, graft failure can be exacerbated by a mismatch in mechanical properties between graft and natural vascular tissue [5,9]. To facilitate endothelial ingrowth and the establishment of a supportive endothelial monolayer, the cells can be directed to migrate into the graft lumen. The use of surface patterns such as microgrooves has been shown to provide sufficient cues to induce both alignment of cell shape and directional cell migration [20]. Therefore, in this present study we incorporated both electrospun microfibers and surface microgrooves in the fabrication of 3D synthetic PU grafts to counteract the mismatch in the graft compliance and to guide the formation of an aligned endothelial monolayer, respectively.

The elasticity of synthetic grafts is important for the grafts to maintain their integrity as pneumatic compliance is one of the major causes of synthetic graft failure post-implantation [5,9,10,31]. The use of electrospun fibers to construct an artificial graft has been shown to be a promising approach to minimize such mismatch in mechanical properties [5]. The Young's moduli of electrospun grafts fabricated from various polymeric materials, such as segmented PU, silk, collagen and poly(lactic-co-glycolic acid), are reportedly 0.54 ± 0.01 MPa [5], 2.45 ± 0.47 MPa [4], 52.3 ± 5.2 MPa [32] and 71 ± 7 MPa [33], respectively. In our study, the longitudinal Young's modulus of electrospun PU graft, 0.43 ± 0.04 MPa, is within the same range as that of natural rabbit aorta (0.50 ± 0.05 MPa), as well as reported values obtained from other polymeric grafts. Although the circumferential modulus of rabbit aorta was not measured in our present study due to the limited sample availability, previous studies show that rabbit [34] and bovine [35] aortae exhibit anisotropic mechanical properties in which the circumferential modulus is significantly higher than the longitudinal modulus. This directional dependence in the modulus can be attributed to the anisotropic arrangement of an elastin network in situ [35]. Thus, our electrospun grafts fabricated with circumferentially aligned microfibers can recapitulate the anisotropic mechanical property of native vessel tissue.

The use of a spin casting technique provides a method to transfer micropatterns from 2D substrata into a 3D arrangement. In our work, microgrooves on PDMS mold can be uniformly imprinted on the luminal surface of a PU graft. The combination of both spin casting and electrospinning techniques allows for the fabrication of a hybrid graft consisting of two distinct structures: microgrooves and microfibers. In contrast to the study of composite vascular grafts [2,11], where the lumen and the exterior consist of different

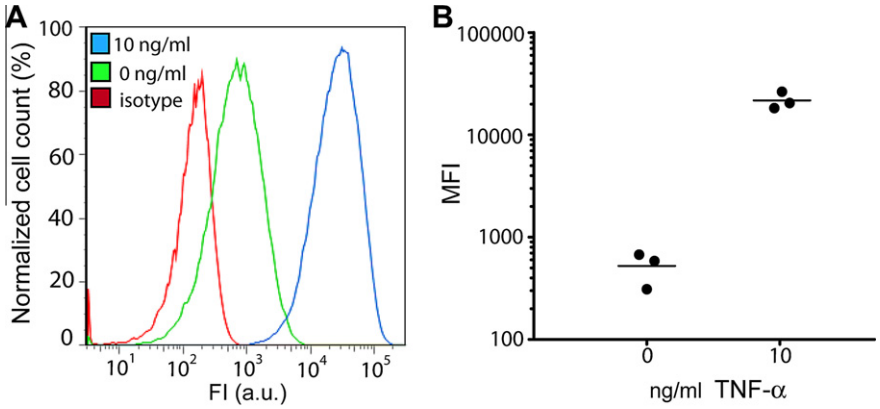

Fig. 6. TNF-α-induced ICAM-1 expression in EA.hy926 endothelial cells grown on PU surfaces. (A) Histogram of fluorescence intensity (FI) of ICAM-1 expression measured by flow cytometry of endothelial cells that were treated with 10 ng ml^{-1} TNF-α (right), 0 ng ml^{-1} TNF-α (middle) and isotype control staining (left). Data are representative of three independent experiments. (B) Plot of the mean fluorescence intensity (MFI) of ICAM-1 staining by TNF-α treated and untreated endothelial cells. Data are the mean of three independent experiments.

polymers, both the microgrooves and the fibrous mesh of our hybrid grafts are fabricated from the same PU solution. Therefore, the combined spin casting and electrospinning techniques may provide a method with which to construct an artificial blood conduit with different microstructures from the same polymeric material.

The alignment of endothelial cells induced by our substrates' contact guidance, either microgrooves or microfibers, is in agreements with previous studies [6,19,29,30]. On 2D surfaces, endothelial cells have been shown to align their shape parallel to arrays of well-defined microgrooves [6], sinusoidal waves [19] and fibers (200 nm to 1 μm in fiber diameter) [7]. In our previous work [6], we found that grooved patterns induced the uniform alignment of endothelial cell monolayers with morphology similar to naturally aligned endothelium under hemodynamic flow. In the present study, we have extended these findings by demonstrating that a groove depth or a fiber diameter of about 1 μm can guide the alignment of endothelial cells inside tubular PU grafts. In addition to the alignment of cell shape, microgrooves may also provide a surface track to induce directional cell migration. Our previous work [20] on endothelial cell migration has shown that microgrooves exert a stronger effect in directing endothelial cell migration over physiological flow (13.5 dyn cm^{-2}). Therefore, both microfibers and microgrooves can potentially improve anastomotic migration of endothelial cells into the midgraft area.

Natural endothelium is functionally responsive to a number of soluble blood-borne signals. In response to pro-inflammatory stimuli such as TNF-α or lipopolysaccharide (LPS), endothelial cells upregulate leukocyte-endothelial cell adhesion molecules such as ICAM-1, VCAM-1 and E-selectin to promote leukocyte adhesion [24,25]. In this study, EA.hy926 endothelial cells cultured on tecothane-derived PU retained the ability to increase ICAM-1 expression (44-fold) when stimulated with TNF-α (Fig. 6). This is in agreement with the study by Williamson et al. [36] that reported an increase in ICAM-1, measured by flow cytometry, in human umbilical vein endothelial cells cultured on polycaprolactone fibers after treatment with LPS. Therefore, in this study we are able to recreate a cytokine-responsive and aligned endothelial monolayer on a synthetic polyurethane surface.

5. Conclusion

Small-diameter PU grafts can be fabricated with uniform micropatterns on their lumens. Using an electrospinning technique, grafts composed entirely of circumferentially aligned microfibers were generated, whereas the combination of both spin casting and electrospinning yielded hybrid grafts with microgrooves on the lumen and nonwoven mesh of microfibers on the exterior. The longitudinal Young's moduli of electrospun and hybrid grafts were shown to be within the same range as native artery. As a response to both micropatterns on the lumens, endothelial cells adopted an elongated cell shape and aligned parallel to the direction of microgrooves and microfibers. At confluence, the aligned endothelial cells expressed VE-cadherin, and could be induced to express ICAM-1 when stimulated with TNF-α. Based on these results, we conclude that electrospinning and spin casting techniques can be used in tandem to fabricate durable, micropatterned, small-diameter polyurethane grafts capable of promoting the formation of aligned endothelial cell monolayers.

Acknowledgements

This research was funded by the Grants in Aid from the Coulter Foundation and the Nanotechnology Institute of Southeastern Pennsylvania. The authors would like to thank Dr. Donald Simons and Mr. Gregory P. Botta for their help in editing the manuscript.

References

[1] Nieponice A, Soletti L, Guan J, Deasy BM, Huard J, Wagner WR, et al. Development of a tissue-engineered vascular graft combining a biodegradable scaffold, muscle-derived stem cells and a rotational vacuum seeding technique. Biomaterials 2008;29:825–33.
[2] Williamson MR, Black R, Kielty C. PCL-PU composite vascular scaffold production for vascular tissue engineering: attachment, proliferation and bioactivity of human vascular endothelial cells. Biomaterials 2006;27:3608–16.
[3] Hong Y, Ye SH, Nieponice A, Soletti L, Vorp DA, Wagner WR. A small diameter, fibrous vascular conduit generated from a poly(ester urethane)urea and phospholipid polymer blend. Biomaterials 2009;30:2457–67.
[4] Soffer L, Wang X, Zhang X, Kluge J, Dorfmann L, Kaplan DL, et al. Silk-based electrospun tubular scaffolds for tissue-engineered vascular grafts. J Biomater Sci Polym Ed 2008;19:653–64.
[5] Matsuda T, Ihara M, Inoguchi H, Kwon IK, Takamizawa K, Kidoaki S. Mechano-active scaffold design of small-diameter artificial graft made of electrospun segmented polyurethane fabrics. J Biomed Mater Res A 2005;73:125–31.
[6] Uttayarat P, Toworfe GK, Dietrich F, Lelkes PI, Composto RJ. Topographic guidance of endothelial cells on silicone surfaces with micro- to nanogrooves: orientation of actin filaments and focal adhesions. J Biomed Mater Res A 2005;75:668–80.
[7] Ma Z, He W, Yong T, Ramakrishna S. Grafting of gelatin on electrospun poly(caprolactone) nanofibers to improve endothelial cell spreading and proliferation and to control cell orientation. Tissue Eng 2005;11:1149–58.
[8] Zilla P, Bezuidenhout D, Human P. Prosthetic vascular grafts: wrong models, wrong questions and no healing. Biomaterials 2007;28:5009–27.
[9] Sarkar S, Salacinski HJ, Hamilton G, Seifalian AM. The mechanical properties of infrainguinal vascular bypass grafts: their role in influencing patency. Eur J Vasc Endovasc Surg 2006;31:627–36.
[10] Soletti L, Hong Y, Guan J, Stankus JJ, El Kurdi MS, Wagner WR, et al. A bilayered elastomeric scaffold for tissue engineering of small diameter vascular grafts. Acta Biomater 2010;6:110–22.
[11] Vaz CM, van Tuijl S, Bouten CV, Baaijens FP. Design of scaffolds for blood vessel tissue engineering using a multi-layering electrospinning technique. Acta Biomater 2005;1:575–82.
[12] Drasler WJ, Wilson GJ, Stenoien MD, Jenson ML, George SA, Dutcher RG, et al. A spun elastomeric graft for dialysis access. ASAIO J 1993;39:114–9.
[13] Li M, Mondrinos MJ, Chen X, Gandhi MR, Ko FK, Lelkes PI. Co-electrospun poly(lactide-co-glycolide), gelatin, and elastin blends for tissue engineering scaffolds. J Biomed Mater Res A 2006;79:963–73.
[14] Del Gaudio C, Bianco A, Folin M, Baiguera S, Grigioni M. Structural characterization and cell response evaluation of electrospun PCL membranes: micrometric versus submicrometric fibers. J Biomed Mater Res A 2009;89:1028–39.
[15] Courtney T, Sacks MS, Stankus J, Guan J, Wagner WR. Design and analysis of tissue engineering scaffolds that mimic soft tissue mechanical anisotropy. Biomaterials 2006;27:3631–8.
[16] Fujimoto K, Minato M, Miyamoto S, Kaneko T, Kikuchi H, Sakai K, et al. Porous polyurethane tubes as vascular graft. J Appl Biomater 1993;4:347–54.
[17] Nishibe T, Okuda Y, Kumada T, Tanabe T, Yasuda K. Enhanced graft healing of high-porosity expanded polytetrafluoroethylene grafts by covalent bonding of fibronectin. Surg Today 2000;30:426–31.
[18] Stankus JJ, Guan J, Fujimoto K, Wagner WR. Microintegrating smooth muscle cells into a biodegradable, elastomeric fiber matrix. Biomaterials 2006;27:735–44.
[19] Jiang X, Takayama S, Qian X, Ostuni E, Wu H, Bowden N, et al. Controlling mammalian cell spreading and cytoskeletal arrangement with conveniently fabricated continuous wavy features on poly(dimethylsiloxane). Langmuir 2002;18:3273–80.
[20] Uttayarat P, Chen M, Li M, Allen FD, Composto RJ, Lelkes PI. Microtopography and flow modulate the direction of endothelial cell migration. Am J Physiol Heart Circ Physiol 2008;294:H1027–35.
[21] Stachelek SJ, Alferiev I, Choi H, Kronsteiner A, Uttayarat P, Gooch KJ, et al. Cholesterol-derivatized polyurethane: characterization and endothelial cell adhesion. J Biomed Mater Res A 2005;72:200–12.
[22] Wulf E, Deboben A, Bautz FA, Faulstich H, Wieland T. Fluorescent phallotoxin, a tool for the visualization of cellular actin. Proc Natl Acad Sci 1979;76:4498–502.
[23] Laschke MW, Strohe A, Scheuer C, Eglin D, Verrier S, Alini M, et al. In vivo biocompatibility and vascularization of biodegradable porous polyurethane scaffolds for tissue engineering. Acta Biomater 2009;5:1991–2001.
[24] Unger RE, Krump-Konvalinkova V, Peters K, Kirkpatrick CJ. In vitro expression of the endothelial phenotype: comparative study of primary isolated cells and cell lines, including the novel cell line HPMEC-ST1.6R. Microvasc Res 2002;64:384–97.
[25] Xue Y, Liu X, Sun J. PU/PTFE-stimulated monocyte-derived soluble factors induced inflammatory activation in endothelial cells. Toxicol In Vitro 2009;24:404–10.
[26] Kanda K, Hayman GT, Silverman MD, Lelkes PI. Comparison of ICAM-1 and VCAM-1 expression in various human endothelial cell types and smooth muscle cells. Endothelium 1998;6:33–44.

[27] Lillie MA, Gosline JM. Mechanical properties of elastin along the thoracic aorta in the pig. J Biomech 2007;40:2214–21.
[28] Weizsacker HW, Pinto JG. Isotropy and anisotropy of the arterial wall. J Biomech 1988;21:477–87.
[29] den Braber ET, de Ruijter JE, Ginsel LA, von Recum AF, Jansen JA. Orientation of ECM protein deposition, fibroblast cytoskeleton, and attachment complex components on silicone microgrooved surfaces. J Biomed Mater Res 1998;40:291–300.
[30] Oakley C, Brunette DM. Topographic compensation: guidance and directed locomotion of fibroblasts on grooved micromachined substrata in the absence of microtubules. Cell Motil Cytoskeleton 1995;31:45–58.
[31] Abbott WM, Megerman J, Hasson JE, L'Italien G, Warnock DF. Effect of compliance mismatch on vascular graft patency. J Vasc Surg 1987;5:376–82.
[32] Matthews JA, Wnek GE, Simpson DG, Bowlin GL. Electrospinning of collagen nanofibers. Biomacromolecules 2002;3:232–8.
[33] Zong X, Ran S, Fang D, Hsiao BS, Chu B. Control of structure, morphology and property in electrospun poly(glycolide-co-lactide) non-woven membranes via post-draw treatments. Polymer 2003;44:4959–67.
[34] Xu Y, Hua TC, Sun DW, Zhou GY. Experimental study and analysis of mechanical properties of frozen rabbit aorta by fracture mechanics approach. J Biomech 2008;41:649–55.
[35] Zou Y, Zhang Y. An experimental and theoretical study on the anisotropy of elastin network. Ann Biomed Eng 2009;37:1572–83.
[36] Williamson MR, Woollard KJ, Griffiths HR, Coombes AG. Gravity spun polycaprolactone fibers for applications in vascular tissue engineering: proliferation and function of human vascular endothelial cells. Tissue Eng 2006;12:45–51.